Chemical Engineering Journal 161 (2010) 60–67

Contents lists available at ScienceDirect

Chemical Engineering Journal

journal homepage: www.elsevier.com/locate/cej

Coagulation efficiency of polyaluminum chloride for natural organic matter removal from low specific UV absorbance surface water and the subsequent effects on chlorine decay

Xiao Zhan, Baoyu Gao*, Qinyan Yue, Yan Wang, Qian Wang

Shandong Key Laboratory of Water Pollution Control and Resource Reuse, School of Environmental Science and Engineering, Shandong University, No. 27 Shanda South Road, Jinan, Shandong 250100, China

ARTICLE INFO

Article history:
Received 19 February 2010
Received in revised form 12 April 2010
Accepted 12 April 2010

Keywords:
Polyaluminum chloride
Natural organic matter removal
Floc strength
Floc regrowth
Floc fractal dimension
Chlorine decay

ABSTRACT

The effect of polyaluminum chloride (PAC) dosage on the coagulation performance and the floc characteristic with respect to the treatment of surface water with low specific UV absorbance (SUVA) value was investigated in this paper. The subsequent effect on chlorine decay was studied by a first decay model and AQUASIM modeling software. The results showed that natural organic matter (NOM) removal increased with the increasing dosage of PAC, while the turbidity removal decreased as the zeta potential further increased to the positive side. At low PAC dosages, charge neutralization was the main mechanism for NOM removal. For the dosage of PAC increased, entrapment, adsorption and complexation played important roles in removing NOM. The growth rate of the flocs was raised with the PAC dosage. Flocs formed at a PAC dosage of 3 mg/L were larger than those at high dosages (12 mg/L and 20 mg/L) and became more compact during the slow stir process. D_f values of flocs with 12 mg/L and 20 mg/L of PAC exhibited a slight decrease at the end of slow stir stage. Floc breakage behavior showed that flocs formed at different dosages of PAC gave different floc strength and the strength factors were in the order: 3 mg/L < 12 mg/L < 20 mg/L. While the floc regrowth factors at different dosages of PAC were in the order: 3 mg/L > 20 mg/L > 12 mg/L. Coagulation treatment with 20 mg/L of PAC resulted in lower chlorine decay rate, but did not lower the total reacting compounds in the effluent when compared with coagulation with the PAC dosage of 12 mg/L. Furthermore, minimal amount of disinfection by-products (DBPs) would be possibly produced after treatment with 12 mg/L of PAC due to the minimal reacting compounds present in the water in this investigation.

1. Introduction

Because of potentially toxic halogenated organics as disinfection by-products (DBPs) produced by natural organic matter (NOM) in drinking water after chlorination [1], research on drinking water treatment shifted from the removal of particle toward the removal of NOM [2]. The characteristics of source water, including the SUVA [3], affect the NOM removal and DBPs formation. The SUVA concentration of the source water varies in different areas, which means that the NOM is quite different in different surface water source [4] and the DBPs concentration should also be different [5]. Coagulation has been widely used for NOM removal in water treatment and is usually used to treat large concentration of NOM [6]. UV absorbance and SUVA were generally shown to correlate well with DBPs formation, especially in waters with relatively high SUVA values [5]. However, there is limited information in the literature on the NOM removal for waters with low SUVA value [5]. These waters may be characterized by having NOM of hydrophilic character and less aromaticity.

As the removal of NOM by coagulation has been extensively researched, more and more interests have been attracted on the floc properties [7,8]. The operational parameters of floc, such as floc strength and floc regrowth after being broken in the coagulation process, have a significant impact on the treatment works. For example, small increases in shear during water works unit processes give rise to floc breakage, reduce floc size, and then lower the removal efficiency [9]. Furthermore the fractal structure and particle size of flocs are generally recognized as two crucial physical properties [10]. The impact of organic matter on floc structure is less well understood. Jarvis [11] has studied the NOM floc physical characteristics. However, for the specific purpose of examining the NOM floc structure in low SUVA surface water, there has been little published as most work has concentrated on flocs from the NOM-rich water or turbidity-dominated water [11,12].

* Corresponding author. Tel.: +86 531 88364832; fax: +86 531 88364513.
E-mail addresses: zhxiao2007@126.com (X. Zhan), bygao@sdu.edu.cn, baoyugao_sdu@yahoo.com.cn (B. Gao), qyyue@sdu.edu.cn (Q. Yue), wangyan@mail.sdu.edu.cn (Y. Wang), mengze_8604@yahoo.com.cn (Q. Wang).

1385-8947/$ – see front matter © 2010 Elsevier B.V. All rights reserved.
doi:10.1016/j.cej.2010.04.023

Table 1
Raw water characteristics and methods of measurement.

Characteristic	Value	How measured
Dissolved organic carbon (DOC) (mg/L)	1.251–1.602	Prefiltered sample measured on a TOC analyzer (Shimadzu, Japan)
Ultraviolet light absorption at 254 nm (UV_{254}) (cm^{-1})	0.044–0.050	Prefiltered sample measured on a UV-754 UV/vis spectrophotometer (Shanghai Jinhua Group Co., Ltd., China)
Turbidity (NTU)	3.32–8.43	Turbidimeter 2100P (Hach, America)
Zeta potential (mV)	−13.7 to −12.3	Zetasizer 3000HSa (Malvern Instruments, UK)
Specific UV absorbance (SUVA) (L/(mg m))	2.87–3.51	SUVA = $\frac{UV_{254}}{DOC} \times 100$

Additionally, in order to comply with DBPs regulations, greater levels of NOM removal is achieved which changes the water quality and then affects the chlorine decay kinetics after dosing chlorine for disinfection. Rossman [13] studied the effects of advanced treatment on the kinetics of chlorine and chloramine decay. While the relationship between dosages of coagulants and the kinetics of chlorine decay has not been well studied.

In this paper, PAC, one form of inorganic polymer coagulants which contains high level of charged polymeric Al hydrolysis products [14,15], was used to treat the surface water with low SUVA value. According to the coagulation efficiency, comparatively investigation was carried out in terms of floc strength and regrowth properties in the coagulation process. The properties of strength and regrowth were measured in terms of response to increasing shear levels through breakage and subsequent regrowth potential. The fractal dimension of the resulting aggregate, which was employed as a measure of the aggregate structure, was determined by small-angle laser light scattering technique (SALLS). The relationship between dosage and chlorine decay process was also discussed. The fast and slow reacting compounds were calculated through a chlorine model and the formation of DBPs was estimated in order to evaluate the treated water quality.

2. Materials and methods

2.1. Preparation of coagulant

PAC with a basicity value (B, OH/Al molar ratio) of 2.0 was synthesized by adding pre-determined amount of Na_2CO_3 slowly into $AlCl_3$ solution under intense agitation. The temperature was kept at $80.0 \pm 0.5\,^{\circ}C$ by using recycling water bath [16]. The total Al content in PAC was determined by titrimetric method according to the national standard of China [17]. The properties of PAC were indicated as follows: total Al (Al_T) content = 0.8605 mol/L, Al_a = 24.8%, Al_b = 32.1%, Al_c = 43.1%, pH = 2.85 ± 0.10. The dosages of PAC are calculated as mg/L of Al during coagulation experiments.

2.2. Raw water

All experiments were carried out on the raw water collected from Queshan reservoir, an important drinking water source in Jinan, China. The raw water characteristics are shown in Table 1, along with the methods of measurement [18]. It is generally indicated that natural waters with high SUVA values, e.g., ≥4 L/(mg m), have relatively high contents of hydrophobic, aromatic and high molecular weight NOM fractions, such as humic substances. This portion of NOM is more readily removed by coagulation [19,20]. In this study, the SUVA of the raw water is less than 4 mg/L, which indicates that the DOC is hydrophilic, non-humic, low in molecular weight, and difficult to be removed. Because of industrial and domestic wastewater discharge, synthetic organic matter has become an important organic matter source in the raw water.

2.3. Coagulation tests

Coagulation experiments were performed on a program-controlled jar test apparatus (ZR4-6, Zhongrun Water Industry Technology Development Co. Ltd., China) containing 1 L samples of water. Water samples were flash mixed at 200 rpm for 1 min and slow mixed at 40 rpm for 15 min. Flocs were allowed to settle for 25 min. At the end of each jar test, the supernatant sample was withdrawn by a syringe from about 2 cm below the water surface for analysis.

2.4. Floc size, breakage and regrowth measurement

Floc size and breakage experiments were performed using an experimental setup similar to Jarvis et al. [21] and also similar to previous work by other authors [22,23]. Coagulation test was carried out on a cylindrical jar tester with a 50 × 40 mm flat paddle impeller. Dynamic floc size was measured during the growth of the flocs using a laser diffraction instrument (Malvern Mastersizer 2000, Malvern, UK). The suspension was monitored by drawing water through the optical unit of the Mastersizer and back into the jar by a peristaltic pump at a flow rate of 2.0 L/h. Size measurements were taken every 0.5 min for the duration of the jar test and logged onto a PC.

After the slow stir phase of coagulation, the effect of increased shear was investigated by increasing the rpm on the jar tester for a further 5 min. Separate experiments were carried out and repeated for rpm of 50, 75, 100, 150, 200, 250 and 300, respectively. Dynamic floc size was measured during growth and breakage of the flocs. The rate at which a floc size decays on exposure to shear is an indication of the floc strength. The empirical relationship between the applied shear and broken floc size which has been used by many researchers to evaluate the floc strength [24–26] was computed as:

$$\log d = \log C - \gamma \log G \tag{1}$$

where d, C, G and γ are the floc diameter (μm), floc strength, average velocity gradient (s^{-1}) and stable floc size exponent, respectively. A modified version with the velocity gradient G being replaced by rpm has also been used by a few researchers [7,8,11,27,28] and was shown as:

$$\log d = \log C' - \gamma' \log \mathrm{rpm} \tag{2}$$

Then, the broken floc size after 5 min shear was plotted against the rpm on a log–log scale, and the slope of this line (γ') gives an indication of the rate of degradation. A larger γ' value is indicative of flocs that are more prone to break into smaller sizes with increasing shear force.

In the floc regrowth tests, flocs were exposed to the shear force at 200 rpm after the slow stir phase was completed. After the breakage phase, the slow stir at 40 rpm was reintroduced for a further 15 min. Floc size was monitored as before. Floc strength and recovery factors, which have previously been used to compare the relative breakage and regrowth of flocs in different flocculated

systems [11,27,29] were calculated as follows:

$$\text{strength factor} = \frac{d_2}{d_1} \times 100 \quad (3)$$

$$\text{recovery factor} = \frac{d_3 - d_2}{d_1 - d_2} \times 100 \quad (4)$$

where d_1 (μm) is the average floc size of the steady phase before breakage, d_2 (μm) is the floc size after the floc breakage period, and d_3 (μm) is the floc size after regrowth to the new steady phase. A larger value of strength factor indicates that flocs are better able to withstand shear, and thus should be considered stronger than the flocs with a lower factor. Likewise, the floc with a larger recovery factor shows better regrowth after high shear.

2.5. Floc fractal dimension

Light scattering method was used here for the determination of aggregate mass fractal dimension. Details in the theory of the mass fractal dimension using SALLS have been reported in a few literatures [30,31]. The light scattering technique involves measurement of light intensity I as a function of the scatter vector Q. The vector is defined as the difference between the incident and scattered wave vectors of the radiation beam in the medium [31], which is given as follows:

$$Q = \frac{4\pi n \sin(\theta/2)}{\lambda} \quad (5)$$

where n, θ, and λ are the refractive index of the medium, the scattered angle, and the wavelength of radiation in vacuum, respectively.

For independently scattering aggregates, the relationship among I, Q and the fractal dimension D_f can be represented by:

$$I \propto Q^{-D_f} \quad (6)$$

D_f can be determined by the slope of a plot of I as a function of Q on a log–log scale. If this gives a straight line, the slope of which is used to give D_f. A larger value of D_f indicates that flocs are compact in the coagulation process.

2.6. Chlorine decay experiments

Chlorine decay experiments were conducted on dark brown bottles to prevent light penetration or algal growth. Thereby the decay of chlorine was due to reducing compounds present in water samples. A chlorine decay study was carried out on two samples of treated water that was chlorinated at two different concentrations (2 mg/L and 2.5 mg/L Cl_2), respectively. The chlorine stock solution was prepared by diluting NaOCl (A.R.) to a final chlorine concentration of 1.5 g/L using deionized water. Free and total chlorine concentrations were measured for 7 days with a free and total chlorine measuring meter HI93711 (Hanna, Italy).

2.7. Chlorine decay model

The simplest model for chlorine decay is the first-order decay model in which the chlorine concentration is assumed to decay exponentially [32,33]. The chlorine decay equation can fairly be presented as follows:

$$\frac{dc}{dt} = -k_b c \quad (7)$$

The integral form is written as:

$$c_t = c_0 \exp(-k_b t) + b \quad (8)$$

where c_t (mg/L) is the chlorine concentration at time t; c_0 (mg/L) is the initial chlorine concentration; k_b (h^{-1}) is the chlorine decay constant and proportional to the rate of chlorine decay; b (mg/L) is the final free chlorine concentration; t (h) is the time.

Moreover, the chlorine decay data obtained were also modeled by AQUASIM to estimate the initial concentrations of reacting compounds [34,35]. The general chlorine decay model includes the following reactions between chlorine and other constituents in the water [36]:

$$Cl_2 + \text{fast reducing agents(organic compounds)}(FRA) \rightarrow \text{inert products} \quad (9)$$

$$Cl_2 + \text{fast reducing nitrogenous compounds}(FRN) \rightarrow \text{combined chlorine} \quad (10)$$

$$Cl_2 + \text{slow reacting agents(organic compounds)}(SRA) \rightarrow \text{inert products} \quad (11)$$

$$Cl_2 + \text{slow reacting nitrogenous compounds}(SRN) \rightarrow \text{combined chlorine}(CC) \quad (12)$$

$$\text{Combined chlorine} \rightarrow \text{inert products} \quad (13)$$

While Cl_2 indicates the available free chlorine present in the water and the sum of Cl_2 and combined chlorine (CC) indicates the total chlorine present in the water. The experimental chlorine decay data were used to estimate the initial concentrations of reacting compounds (*FRN*, *SRN*, *FRA* and *SRA*).

3. Results and discussions

3.1. Effect of PAC dosages on the coagulation performance

The effects of PAC dosages on NOM and turbidity removal as well as the zeta potentials were shown in Fig. 1. The various removals of DOC and UV_{254} with dosages showed the similar trends: DOC and UV_{254} removals increased with the PAC dosage increasing and the increasing rate became slowly when the dosage was high. The zeta potential of the raw water was less than −13 mV and the turbidity was close to 5 NTU. When the PAC dosage was less than 3 mg/L, the zeta potential of the flocs increased rapidly with the dosage, and meanwhile the turbidity removal efficiency increased sharply. However, as the PAC dosage was greater than 3 mg/L, the zeta potential grew up slightly and the turbidity remained approximately constant. When the dosage was further increased and greater than 10 mg/L, the zeta potential was still increased, however, turbidity removals began to decrease gradually.

Istv'an [37] proposed that the hydrolysis of metal ions occurred immediately after contacting with water. After added to water, PAC rapidly undergoes hydrolysis reactions to form other dissolved Al species or Al-hydroxide precipitates [38]. At the low dosage of PAC, aluminum hydroxide precipitation was minimal. Charge neutralization was the mechanism used to explain the precipitation of NOM [39]. Positive aluminum interacts electrostatically with anionic NOM to form insoluble charge neutral products. This mechanism was effective on removing the colloidal and higher molecular weight NOM, which could act as nuclei for precipitate formation. When the concentration of PAC was high enough to cause rapid precipitation of $Al(OH)_3$, NOM can be removed by surface adsorption. Additionally, a small portion of Al reacted with NOM to form Al–NOM complex [38,40]. The complex of metal cation and NOM

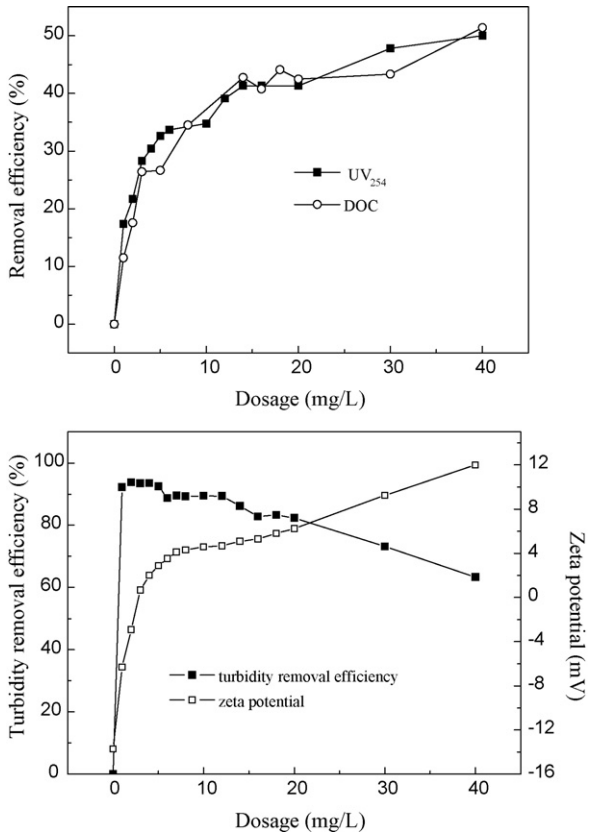

Fig. 1. UV_{254}, DOC and turbidity removal efficiency along with the zeta potentials by coagulation as a function of PAC dosage.

remained in solution until either the binding capacity of the NOM has been saturated or the solubility of the metal–NOM complex was exceeded.

On the other hand, the removal of NOM was favored at acid range. It is worth noticing that the solution pH dropped toward the acid range with high dosage. For example, after coagulation, the pH of the effluent was 6.96 for the PAC dosage of 40 mg/L, 7.56 for the dosage of 3 mg/L. This may be another reason for the high NOM removal efficiency at high PAC dosage [14,41,42].

It was noted that turbidity removal efficiency reached the optimal values when zeta potential was close to the isoelectric point where the charge neutralization was the main mechanism as mentioned above. As the dosage was excessive, further PAC hydrolysis led to the formation of polymer bridges between particle, which bridged the particle and destabilized Al–NOM complex and caused the particles to repel each other [43,44]. Thus, the turbidity removal efficiency decreased as the dosage further increased.

Fig. 2 showed the variation of SUVA value as a function of the coagulant dosage. It was found that the SUVA value of the treated water was less than that of the raw water at low dosage of PAC and increased when the dosage was greater than 5 mg/L. Coagulation preferentially removed high molecular weight and hydrophobic fractions of organic matter. At low dosage of PAC, the high molecular weight organic matter was removed. The hydrophobic fractions were low and the SUVA value was slightly decreased. As the dosage of PAC was increased, the hydrophilic fractions were then gradually removed, resulting in higher SUVA values.

3.2. Floc size

The flocs' size and structure may be affected significantly by the dosage of coagulant [27]. Floc formation kinetics was investi-

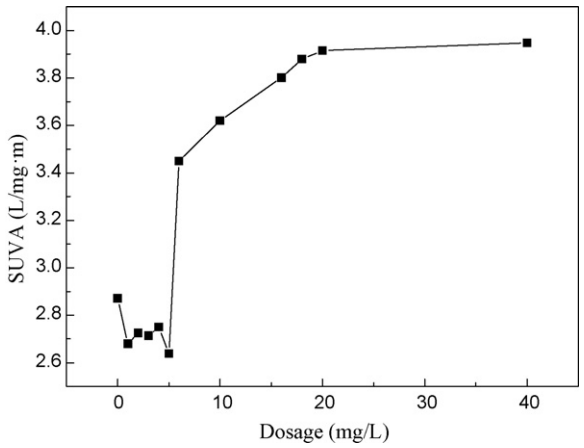

Fig. 2. SUVA values by coagulation as a function of PAC dosage.

gated and the results were shown in Fig. 3. The median equivalent volumetric diameter (d_{50}) was selected as the respective floc size, although, the same trends were seen for the whole range of floc sizes investigated.

The general trend showed that when the dosage of PAC was less than 3 mg/L, floc size was seen to increase as the dosage increased. The flocs at a dosage of 3 mg/L reached a maximum size of 800 μm. A substantial reduction in floc size was seen for the dosage of 12 mg/L and 20 mg/L as the maximum floc size approached 350 μm and 200 μm, respectively. At high dosages (12 mg/L and 20 mg/L), the floc size presented a slight decrease at the end of the slow stir, which could be explained by the surface erosion of flocs during coagulation.

Flocs formed more quickly at higher dosage. The growth rate of the flocs was much quicker for the floc at a dosage of 20 mg/L with the maximum size being reached between 2 min and 4 min. Flocs at a dosage of 1 mg/L gave much lower growth rate and the peak flocs did not appear within the coagulation time. In the coagulation process, efficient collisions were increased as the increase in PAC dosage. More particles were destabilized throughout efficient collisions, which led to abrupt increase of the aggregation rate at the initial aggregation. Thus, the growth rate of the flocs was raised with dosage. At a high dosage, microflocs became positive (zate potentials results in Fig. 1) and repel each other [43,44], which hampered the aggregation of flocs and reduced the floc size.

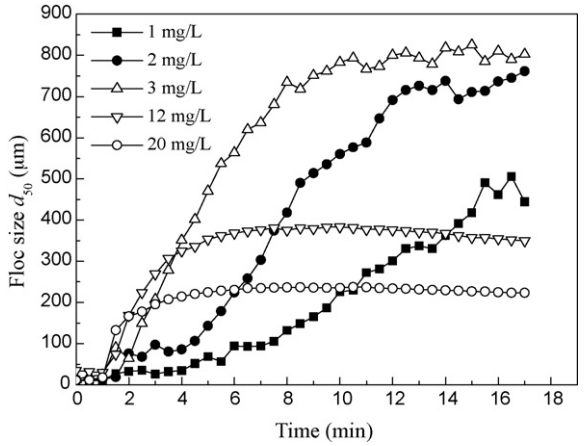

Fig. 3. The growth rates of flocs for coagulation as a function of PAC dosage.

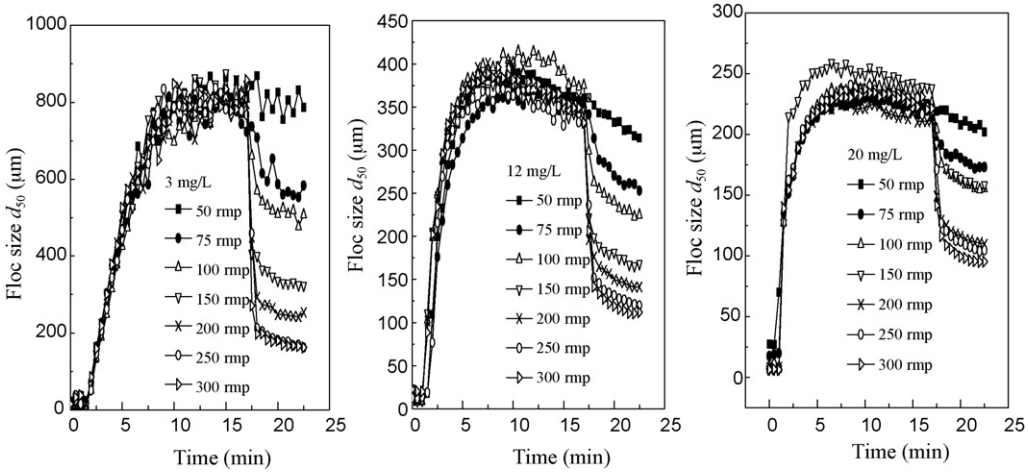

Fig. 4. The growth and breakage profile of flocs with increasing rpm at three dosages of PAC.

3.3. Floc breakage

After the flocs had reached their steady state size at the end of slow stir period, they were exposed to increased shears. The change of floc size versus coagulation time was shown in Fig. 4.

It can be seen that the floc d_{50} decreased with increasing shear rate and the response of the floc d_{50} were similar for the three dosages of PAC. At low rpms (50 and 75), there was only a gradual decline in floc size. At an rpm of 100 and above, a significant drop in floc d_{50} can be seen immediately after the introduction of increased shear, and then followed by a gradual decline. Then, these observations were quantified in Fig. 5 according to Eq. (2) to compare the difference of the three dosages in the response of floc d_{50} to increased shear. As mentioned above, the slope (γ') of this line gives an indication of floc size degradation rate. The smaller the gradient of the slope, the stronger the floc. It can be seen that a PAC dosage of 20 mg/L gave a more gently decrease in floc size than other two dosages with the increase of rpm, as reflected by the lowest value of γ' (0.42). Thus the flocs were far more resistant on exposure to increased shear. The next largest floc decrease in size was obtained by a dosage of 12 mg/L ($\gamma' = 0.60$). A dosage of 3 mg/L gave the most rapid drop in floc size and the highest γ' value (0.88). Larger flocs become more affected by the microscale eddied that are attributed to floc breakage. At small sizes, flocs are more likely to become entrained within eddies rather than be broken by them [45]. This may explain why large flocs formed at 3 mg/L of PAC were broken more extensively.

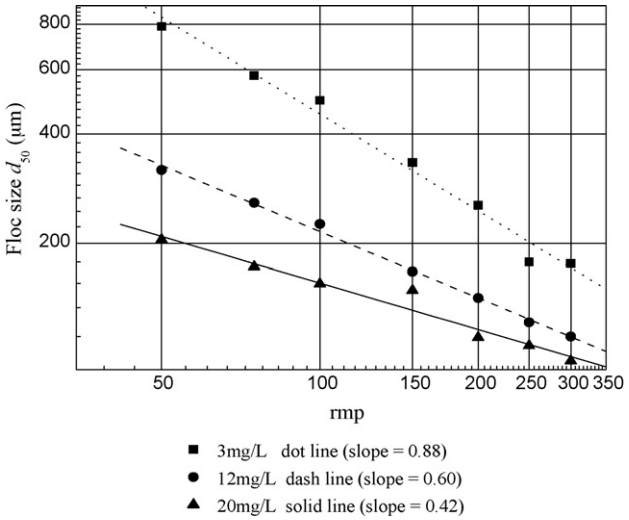

Fig. 5. Floc breakage rates at three dosages of PAC.

3.4. Floc strength and recovery

In the case of 5 min shear period, the floc breakage could be observed and the floc size decreased for all the three dosages of PAC. As the shear was reduced again, the flocs began to regrow. The strength and recovery factors of shear (200 rpm) on floc breakage and regrowth for d_{50} were summarized in Table 2.

In the case of 5 min shear period, the d_{50} size of the flocs after shear was about 250 μm for a dosage of 3 mg/L. Flocs with 12 mg/L and 20 mg/L PAC were broken into smaller floc sizes of around 140 μm and 110 μm, respectively. It can be seen that 12 mg/L and 20 mg/L flocs did not generally break to the same extent as larger flocs at a dosage of 3 mg/L. After 15 min of regrowth, the d_{50} size of the flocs after shear was about 450 μm, 180 μm and 130 μm for PAC dosage of 3 mg/L, 12 mg/L and 20 mg/L, respectively. The strength and recovery factor for d_{50} were summarized in Table 2. Flocs at a PAC dosage of 20 mg/L were better able to resist shear with the floc strength factor of 50. Flocs formed at 3 mg/L of PAC were poor to resistant increasing sheer with the lowest strength factor of 32. There were not enough physical bonds between the flocs formed under charge neutralization, thus, the flocs formed at a dosage of 3 mg/L were the weakest and the size decreased sharply with the shear force. While the floc strength formed under a PAC dosage of 20 mg/L was the strongest, which could be ascribed to the strong bonds of polymer chains. The result was consistent with that obtained in the "floc breakage" section of this paper.

Flocs with a PAC of 3 mg/L were able to regrow after the increasing sheer with the recovery factor of 35. The regrowth capacities of flocs under different dosages were in the following order: flocs with 3 mg/L of PAC > flocs with 20 mg/L of PAC > flocs with 12 mg/L of PAC. Previous research has reported that recoverability of flocs gives some indication of the floc internal bonding structure [7]. The flocs formed by charge neutralization should give total recoverability [46], while sweep flocs give poor regrowth after breakage [47].

Table 2
Strength and recovery factors of flocs (d_{50}) after 5 min of breakage followed by regrowth for 15 min.

Dosage of PAC (mg/L)	3	12	20
Strength factor	32	38	50
Recovery factor	35	18	22

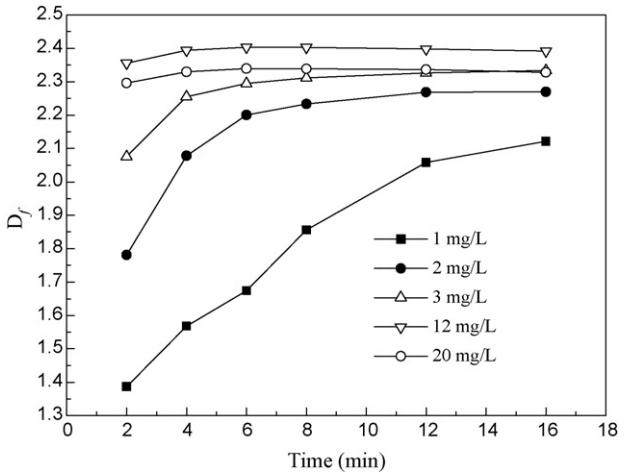

Fig. 6. Fractal dimensions (D_f) of flocs during coagulation process as a function of PAC dosage.

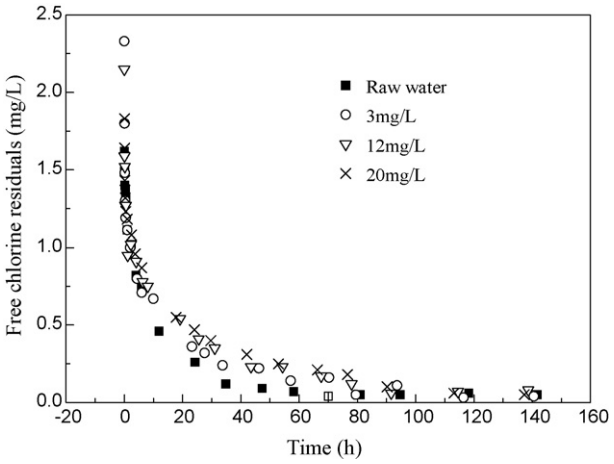

Fig. 7. Free chlorine decay profile for raw water and treated water by PAC (chlorine 2.0 mg/L (as Cl_2)).

This is the possible reason why flocs at 3 mg/L of PAC showed better regrow ability after the increasing sheer than the flocs at 20 mg/L of PAC.

3.5. Fractal dimension

The fractal dimension (D_f) of the flocs formed by PAC coagulation at various dosages were presented in Fig. 6. When the PAC dosage was less than 3 mg/L, D_f was raised with the increasing dosage. That was because, at the low dosage, increasing PAC significantly reduced the interior repulsion of flocs, which contributed to the formation of compacted flocs [48]. From the analysis of the entire coagulation process, a continuous and gentle increase in D_f could be seen as the increase of coagulation time for a PAC dosage of less than 3 mg/L, and the D_f values reached the maximum at the end of slow stir stage, which suggested that the floc structures become more compact during the coagulation process. A possible reason was that floc structure became more compact and stable by restructuring and rearrangement [49]. In addition, the rupture of weak points under prolonged mixing and shear conditions also contributes to the formation of a homogeneous and dense floc structure [50]. D_f value of flocs at a dosage of 20 mg/L was much lower than that of flocs with a dosage of 12 mg/L. As the dosage further increased (from 12 mg/L to 20 mg/L), polymer bridges enhanced which resulted in the formation of open-structure flocs. For high dosages of 12 mg/L and 20 mg/L, D_f value increased at the initial aggregation, but a gentle decrease in D_f values could be seen at the end of slow stir stage, which could be explained by the breakage of flocs during coagulation. The flocs with high dosages contained large porosity and then were easily broken by surface erosion of eddies splitting (i.e. large-scale fragment) [21].

3.6. Effect of dosages on chlorine decay

Chlorine with an initial concentration of 2.0 mg/L (as Cl_2) was added to the treated water with three dosages of PAC. Degradations of free chlorine residuals were presented in Fig. 7. A higher degradation rate was observed in the solution at the first 10 h and the residual chlorine became changing slightly after 10 h. The rapid and slow decay rates are likely due to different competing reactants, such as the oxidation of inorganic compounds (rapid) and substitution reactions with NOM (relatively slow).

The decay constants of first-order chlorine decay equation were given in Table 3 along with the quality of the treated water. Treated water by different dosages of PAC obtained different chlorine degradation rates and the order of degradation rate were: 20 mg/L < 12 mg/L < 3 mg/L by studying the value of K_b. Different chlorine decay rate may due to the charge density of aggregation [51]. Zeta potential of the effluent after coagulation at a PAC dosage of 20 mg/L was positive and the value was 6.24 mV which was higher than that of the other effluents. Although the electrostatic attraction was large between OCl^- and the aggregation the reactivity of OCl^- with NOM was less influenced by the attraction. It is proposed that more NOM was entrapped in the aggregates at a PAC dosage of 20 mg/L and could not contact with chlorine, which inhibited the reaction between chlorine and the organics that has been entrapped in the aggregates.

As shown in Table 3, the water quality improved significantly after the coagulation. Though aromatic compounds of NOM were more preferentially removed by coagulation, the small aromatic molecules and linear molecular matter was difficult to remove which may easily react with chlorine to form DBPs [29]. A higher residual DOC in the sample resulted in greater potential to form DBPs [52]. After coagulation at a PAC dosage of 3 mg/L, there were more residual DOC in the effluent which would react with chlorine after dosing chlorine. So there was less free chlorine and more DBPs would be produced during the reaction between chlorine and NOM.

The effluent after treatment with 12 mg/L of PAC contained maximum amount of final free chlorine residuals by comparing the value of *b*. More free chlorine residuals indicated that there were less NOM to consume chlorine. The result was in accordance with the DOC value which indicated that the effluent contained less NOM.

When the PAC dosage was 20 mg/L, the colloidal floc came into being because of the electrostatic repulsion. The colloidal flocs cannot settle down in the jar test apparatus after the PAC coagulation process, but it can be filtered off by filtration through 0.45 μm filtration membrane [39]. Though the DOC at a dosage of 20 mg/L which was measured by filtered through 0.45 μm membrane was low, the NOM and turbidity was higher in the effluent than that at a dosage of 12 mg/L. Therefore, the effluent with 20 mg/L of PAC contained less DOC, but there were less free chlorine remained.

Values for various fast and slow reacting nitrogenous and organic compounds were provided in Table 4, as estimated by the chlorine decay model using AQUASIM modeling software. Coagulation with PAC was effective in removing fast reacting compounds. *FRN* and *FRA* were reduced with increased PAC dosage. Coagulation with 12 mg/L of PAC removed more *SRN* and *SRA*, while *SRN* and *SRA* were increased at 20 mg/L of PAC. The highest removal efficiency

Table 3
Fitted equations of chlorine decay and the characteristics of raw water and treated water.

Dosage of PAC (mg/L)	Fitting equation	R^2	Turbidity (NTU)	UV_{254} (cm^{-1})	DOC (mg/L)	pH	Zeta (mV)
Raw water	–	–	3.82	0.044	1.602	7.78	−13.0
3	$y = 1.46 \times \exp(-x/4.93) + 0.18$	0.880	0.50	0.034	1.179	7.76	0.66
12	$y = 1.33 \times \exp(-x/7.18) + 0.20$	0.883	0.60	0.028	0.7861	7.56	4.68
20	$y = 1.27 \times \exp(-x/12.13) + 0.17$	0.936	0.82	0.027	0.6895	7.54	6.24

Table 4
The initial concentrations of reacting compounds.

Dosage (mg/L)	*FRN* (mg/L)	*SRN* (mg/L)	*FRA* (mg/L)	*SRA* (mg/L)	Initial chlorine demand (*FRN* and *FRA*)	Constant chlorine demand (*SRN* and *SRA*)	Total chlorine demand
Raw water	2.856	0.287	0.183	2.424	3.039	2.711	5.750
3	0.294	0.010	0.342	2.592	0.636	2.602	3.238
12	0.108	0.274	0.090	1.650	0.198	1.924	2.122
20	0.009	0.404	0.050	2.560	0.059	2.964	3.023

in total chlorine demand was achieved at a PAC dosage of 12 mg/L and the efficiency was up to 63%.

Studies have presented that coagulants preferentially remove hydrophobic material but are relatively poor at removing hydrophilic, low molecular weight organics [53]. Shin et al. [54] reported that low molecular weight NOM were prone to form DBPs. Thus, most *SRN* and *SRA* were probably compounds with low molecular weight and were hydrophilic. Then, a PAC dosage of 12 mg/L which could reduce *SRN* and *SRA* to a large extent would lower the formation of DBPs. The result was consistent with that found from the free chlorine residuals mentioned above. Increasing PAC dosage (20 mg/L) would generate fine flocs which were more prone to suspend in the supernatant and thus might result in lower removal efficiencies of *SRN* and *SRA* although the DOC removal efficiency was slightly higher than that of a dosage of 12 mg/L.

4. Conclusions

A series of experimental procedures were developed to study the coagulation behavior and floc characteristic with respect to the treatment of surface water with low SUVA. The effect of coagulant dosage on the chlorine decay performance was investigated as well as estimating the various reacting compounds using AQUASIM modeling software. The main conclusions from this work were listed as the following:

(1) NOM removal was increased with the increasing dosage of PAC. The SUVA value decreased initially due to the low content of hydrophobic organic fractions and increased when the hydrophilic fractions were gradually removed. The turbidity removal was increased at a low PAC dosage where charge neutralization was the main coagulation mechanism, but decreased as the zeta potential further increased to the positive side, where entrapment, adsorption and complexation played important roles in treating the surface water.
(2) The growth rate of the flocs was raised with the PAC dosage. The floc size was increased for the dosage of less than 3 mg/L and sharply decreased for PAC dosage of 12 mg/L and 20 mg/L. Large flocs formed at a PAC dosage of 3 mg/L were easily broken by the increasing sheers, but able to regrow after the sheers. Small flocs with a 20 mg/L of PAC gave better resistance to the increasing sheers but poor recoverability.
(3) Flocs with a dosage of 3 mg/L became more compact during the slow stir process. For high dosage of 12 mg/L and 20 mg/L, D_f value increased at the initial aggregation, but decreased at the end of slow stir stage. As the dosage was increased from 12 mg/L to 20 mg/L, the flocs became more open and less compact resulted in D_f decreasing.
(4) The coagulated effluent at a PAC dosage of 12 mg/L would possibly produce minimal amount of DBPs due to the minimal reacting compounds present in the water and contained the maximum free chlorine residuals. A PAC dosage of 20 mg/L achieved a lower chlorine degradation rate. Though less DOC retained in the treated effluent, coagulation treatment with 20 mg/L of PAC resulted in less free chlorine residuals and more total reacting compounds in the effluent when compared with coagulation with the dosage of 12 mg/L.

Acknowledgements

This work is supported by the National Major Special Technological Programmes Concerning Water Pollution Control and Management in the Eleventh Five-year Plan Period (2008ZX07422-003-02), Key Projects in the National Science & Technology Pillar Program in the Eleventh Five-year Plan Period (2006BAJ08B05-2) and the National Natural Science Foundation of China (50808114). The kind suggestions from the reviewers are greatly acknowledged.

References

[1] J.J. Rook, Formation of haloforms during chlorination of natural waters, Water Treat. Exam. 28 (1974) 234–243.
[2] M.J. Semmens, T.K. Field, Coagulation experiences in organics removal, J. Am. Water Works Assoc. 72 (1980) 476–483.
[3] D.M. Owen, G.L. Amy, Z.K. Chowdhury, Characterization of Natural Organic Matter and its Relationship to Treatability, American Water Works Association Research Foundation, Denver, Colorado, 1993.
[4] C. Chen, X. Zhang, L. Zhu, J. Liu, W. He, H. Han, Disinfection by-products and their precursors in a water treatment plant in North China: seasonal changes and fraction analysis, Sci. Total Environ. 397 (2008) 140–147.
[5] N. Ates, M. Kitis, U. Yetis, Formation of chlorination by-products in waters with low SUVA—correlations with SUVA and differential UV spectroscopy, Water Res. 41 (2007) 4139–4148.
[6] A. Moncayo-Lasso, C. Pulgarin, N. Benítez, Degradation of DBPs' precursors in river water before and after slow sand filtration by photo-Fenton process at pH 5 in a solar CPC reactor, Water Res. 42 (2008) 4125–4132.
[7] P. Jarvis, B. Jefferson, S.A. Parsons, Breakage, regrowth, and fractal nature of natural organic matter flocs, Environ. Sci. Technol. 39 (2005) 2307–2314.
[8] E.L. Sharp, P. Jarvis, S.A. Parsons, B. Jefferson, The impact of zeta potential on the physical properties of ferric-NOM flocs, Environ. Sci. Technol. 40 (2006) 3934–3940.
[9] M. Boller, S. Blaser, Particles under stress, Water Sci. Technol. 37 (1998) 9–29.
[10] K.W. Chau, Investigation on effects of aggregate structure in water and wastewater treatment, Water Sci. Technol. 50 (2004) 119–124.
[11] P. Jarvis, B. Jefferson, S.A. Parsons, Floc structural characteristics using conventional coagulation for a high doc, low alkalinity surface water source, Water Res. 40 (2006) 2727–2737.
[12] J. Gregory, Proceedings of the Nano and Micro Particles in Water and Wastewater Treatment Conference, International Water Association, Zurich, 2003.
[13] L.A. Rossman, The effect of advanced treatment on chlorine decay in metallic pipes, Water Res. 40 (2006) 2493–2502.
[14] D.S. Wang, W. Sun, Y. Xu, H.X. Tang, J. Gregory, Speciation stability of inorganic polymer flocculant—PACl, Colloids Surf. A 243 (2004) 1–10.

[15] M.Q. Yan, D.S. Wang, J.H. Qu, W.J. He, C.W.K. Chow, Relative importance of hydrolyzed Al(III) species (Ala, Alb and Alc) during coagulation with polyaluminum chloride: a case study with the typical micro-polluted source waters, J. Colloid Interface Sci. 316 (2007) 482–489.
[16] B.Y. Gao, Y.B. Chu, Q.Y. Yue, B.J. Wang, S.G. Wang, Characterization and coagulation of a polyaluminum chloride (PAC) coagulant with high Al13 content, J. Environ. Manage. 76 (2005) 143–147.
[17] GB15892-1995, Water Treatment Chemicals-Polyaluminum Chloride, National Standards of the People's Republic of China, (in Chinese).
[18] J.C. Wei, B.Y. Gao, Q.Y. Yue, Y. Wang, L. Lu, Performance and mechanism of polyferric-quaternary ammonium salt composite flocculants in treating high organic matter and high alkalinity surface water, J. Hazard. Mater. 165 (2009) 789–795.
[19] J.K. Edzwald, W.C. Becker, K.L. Wattier, Surrogate parameters for monitoring organic matter and THM precursor, J. Am. Water Works Assoc. 77 (1985) 122–131.
[20] J.L. Weishaar, G.R. Aiken, B.A. Bergamaschi, M.S. Fram, R. Fujii, Evaluation of specific ultra-violet absorbance as an indicator of the chemical composition and reactivity of dissolved organic carbon, Environ. Sci. Technol. 37 (2003) 4702–4708.
[21] P. Jarvis, B. Jefferson, J. Gregory, S.A. Parsons, A review of floc strength and breakage, Water Res. 39 (2005) 3121–3137.
[22] C.A. Biggs, P.A. Lant, Activated sludge flocculation: on-line determination of floc size and the effect of shear, Water Res. 34 (2000) 2542–2550.
[23] P.T. Spicer, S.E. Pratsinis, J. Raper, R. Amal, G. Bushell, G. Meesters, Effect of shear schedule on particle size, density, and structure during flocculation in stirred tanks, Powder Technol. 97 (1998) 26–34.
[24] J. Leentvaar, M. Rebhun, Strength of ferric hydroxide flocs, Water Res. 17 (1983) 895–902.
[25] R.J. Francois, Strength of aluminium hydroxide flocs, Water Res. 21 (1987) 1023–1030.
[26] D.H. Bache, E. Rasool, D. Moffat, F.J. McGilligan, On the strength and character of alumino-humic flocs, Water Sci. Technol. 40 (1999) 81–88.
[27] P. Jarvis, B. Jefferson, S.A. Parsons, How the natural organic matter to coagulant ratio impacts on floc structural properties, Environ. Sci. Technol. 39 (2005) 8919–8924.
[28] M.A. Yukselen, J. Gregory, The reversibility of floc breakage, Int. J. Miner. Process. 73 (2004) 251–259.
[29] C. Musikavong, S. Wattanachira, T.F. Marhaba, P. Pavasant, Reduction of organic matter and trihalomethane formation potential in reclaimed water from treated industrial estate wastewater by coagulation, J. Hazard. Mater. 127 (2005) 58–67.
[30] G.C. Bushell, Y.D. Yan, D. Woodfield, J. Raper, R. Amal, On techniques for the measurement of the mass fractal dimension of aggregates, Adv. Colloid Interface Sci. 95 (2002) 1–50.
[31] J. Guan, T.D. Waite, R. Amal, Rapid structure characterization of bacterial aggregates, Environ. Sci. Technol. 32 (1998) 3735–3742.
[32] F. Hua, J.R. West, R.A. Barker, C.F. Forster, Modelling of chlorine decay in municipal water supplies, Water Res. 33 (1999) 2735–2746.
[33] D.L. Boccelli, M.E. Tryby, J.G. Uber, R.S. Summers, A reactive species model for chlorine decay and THM formation under rechlorination conditions, Water Res. 37 (2003) 2654–2666.
[34] V. Jegatheesan, S.H. Kim, C.K. Joo, B. Gao, Evaluating the effects of granular and membrane filtrations on chlorine demand in drinking water, J. Environ. Sci. 21 (2009) 23–29.
[35] G. Kastl, I. Fisher, V. Jegatheesan, Evaluation of chlorine decay kinetics expressions for drinking water distribution systems modelling, J. Water SRT Aqua. 48 (1999) 219–226.
[36] K. Bell-Ajy, M. Abbaszadegan, E. Ibrahim, D. Verges, M. LeChevallier, Conventional and optimized coagulation for NOM removal, J. Am. Water Works Assoc. 92 (2000) 44–58.
[37] L. Istv'an, On the type of bond developing between the aluminum and iron (III) hydroxide and organic substances, Water Sci. Technol. 27 (1993) 242–252.
[38] J.E. Van Benschoten, J.K. Edzwald, Chemical aspect of coagulation using aluminum salts. I: hydrolytic reactions of alum and polyaluminum chloride, Water Res. 24 (1990) 1519–1526.
[39] M.Q. Yan, D.S. Wang, J.R. Ni, J.H. Qu, C.W.K. Chow, H.L. Liu, Mechanism of natural organic matter removal by polyaluminum chloride: effect of coagulant particle size and hydrolysis kinetics, Water Res. 42 (2008) 3361–3370.
[40] J.E. Gregor, C.J. Nokes, E. Fenton, Optimising natural organic matter removal from low turbidity waters by controlled pH adjustment of aluminum coagulation, Water Res. 31 (1997) 2949–2958.
[41] M.Q. Yan, D.S. Wang, J.H. Qu, J.R. Ni, C.W.K. Chow, Enhanced coagulation for high alkalinity and micro-polluted water: the third way through coagulant optimization, Water Res. 42 (2008) 2278–2286.
[42] M.Q. Yan, D.S. Wang, J.F. Yu, J.R. Ni, M. Edwards, J.H. Qu, Enhanced coagulation with polyaluminum chlorides: role of pH/alkalinity and speciation, Chemosphere 71 (2008) 1665–1673.
[43] C.R. O'Melia, Particle–particle interactions, in: W. Stumm (Ed.), Aquatic Surface Chemistry, Wiley–Interscience, New York, 1987.
[44] J. Gregory, Fundamentals of flocculation, CRC Crit. Rev. Environ. Control 19 (1989) 185–230.
[45] D.S. Parker, W.J. Kaufman, D. Jenkins, Floc breakup in turbulent flocculation processes, J. Sanit. Eng. Div., Am. Soc. Civ. Eng. 1 (1972) 79–99.
[46] V. Chaignon, B.S. Lartiges, A.E. Samrani, C. Mustin, Evolution of size distribution and transfer of mineral particles between flocs in activated sludges: an insight into floc exchange dynamics, Water Res. 36 (2002) 484–676.
[47] M.I. Aguilar, J. Sáez, M. Lloréns, A. Soler, J.F. Ortuño, Microscopic observation of particle reduction in slaughterhouse wastewater by coagulation–flocculation using ferric sulphate as coagulant and different coagulant aids, Water Res. 37 (2003) 2233–2241.
[48] J.C. Wei, B.Y. Gao, Q.Y. Yue, Y. Wang, W.W. Li, X.B. Zhu, Comparison of coagulation behavior and floc structure characteristic of different polyferric-cationic polymer dual-coagulants in humic acid solution, Water Res. 43 (2009) 724–732.
[49] C. Selomulya, R. Amal, G. Bushell, T.D. Waite, Evidence of shear rate dependence on restructuring and breakup of latex aggregates, J. Colloid Interface Sci. 236 (2001) 66–77.
[50] D.C. Hopkins, J.J. Ducoste, Characterizing flocculation under heterogeneous turbulence, J. Colloid Interface Sci. 264 (2003) 184–194.
[51] Q. Ji, H. Liu, C. Hu, J. Qu, D. Wang, J. Li, Removal of disinfection by-products precursors by polyaluminum chloride coagulation coupled with chlorination, Sep. Purif. Technol. 62 (2008) 464–469.
[52] J. van Leeuwen, R. Daly, M. Holmes, Modeling the treatment of drinking water to maximize dissolved organic matter removal and minimize disinfection by-product formation, Desalination 176 (2005) 81–89.
[53] D.A. Fearing, J. Banks, S. Guyetand, C.M. Eroles, B. Jefferson, D. Wilson, P. Hillis, A.T. Campbell, S.A. Parsons, Combination of ferric and MIEX® for the treatment of humic rich water, Water Res. 38 (2004) 2551–2558.
[54] H.S. Shin, J.M. Monsallier, G.R. Choppin, Spectroscopic and chemical characterizations of molecular size fractionated humic acid, Talanta 50 (1999) 641–647.